Determination of Viscoelastic Properties of human Carotid Atherosclerotic Plaque by Inverse Boundary Value Analysis

Determination of Viscoelastic Properties of human Carotid Atherosclerotic Plaque by Inverse Boundary Value Analysis

Xiaochang Leng[1,a,*], Boran Zhou[2,b], Xiaomin Deng[3,c], Lindsey Davis[4,d], Michael A. Sutton[3,4,e], Tarek Shazly[3,4,f] and Susan M. Lessner[4,5,g]

[1]Institute of Engineering Mechanics, Nanchang University, Jiangxi, 330031, People's Republic of China
[2]Department of Radiology, Mayo Clinic, Rochester, MN 55905
[3]College of Engineering and Computing, Department of Mechanical Engineering, University of South Carolina, Columbia, SC 29208
[4]College of Engineering and Computing, Biomedical Engineering Program, University of South Carolina, Columbia, SC 29208
[5]School of Medicine, Department of Cell Biology & Anatomy, University of South Carolina, Columbia, SC 29208
Email: [a]lengxc1984@163.com, [b]zhou.boran@mayo.edu, [c]DENG@cec.sc.edu, [d]davis79@email.sc.edu, [e]sutton@sc.edu, [f]shazly@cec.sc.edu, [g]susan.lessner@uscmed.sc.edu

Abstract. In this study, we assessed the mechanical response of samples from human atherosclerotic diseased media and fibrous cap via uniaxial tensile testing. Results show a pronounced hysteresis phenomenon caused by viscoelasticity during the loading-unloading process. An inverse analysis method with finite element modeling was employed to identify the material parameter values for a viscoelastic anisotropic (VA) constitutive model through matching simulation predictions of load-displacement curves with experimental measurements. The identified material parameter values can be used in simulation studies of diseased human carotid arteries, including investigations of inflation processes associated with stenting or angioplasty.

1. Introduction

Atherosclerotic plaque rupture is the main cause of acute cardiovascular events such as myocardial infarction and stroke, which cause life-threatening consequences [1, 2]. Plaque rupture is a complicated process involving interactions among the arterial wall, blood pressure, flow-induced shear stress on the fibrous cap, and clinical interventions (stenting and angioplasty).

Finite element modeling has been used in the analysis of the fibrous cap failure phenomenon to evaluate stress, strain and damage and to assess the vulnerability of the plaque tissue under supraphysiological expansion [3] . Numerical predictions of the mechanical behavior of plaque tissue are dependent on the availability of material properties, including viscoelastic properties. The instantaneous maximum stresses inside the plaque tissue are governed by viscoelasticity, which tends to reduce the degree of damage under dramatic and large deformation conditions. The viscoelastic response of arterial tissues plays an important role in the interaction between the arterial wall and vasoactive drugs, hypertension, or vascular trauma [4, 5]. Given the complicated interaction modalities and the biomechanical behavior of diseased vascular tissues during clinical interventions, there is a pressing need to characterize the viscoelastic properties of atherosclerotic plaque tissues.

In this study, uniaxial tension experiments on human carotid plaque diseased media and fibrous caps were performed. A viscoelasticity formulation by Holzapfel [6] was incorporated into the Holzapfel-Gasser-Ogden (HGO) hyperelasticity model [7], leading to the development of a viscoelastic anisotropic (VA) model for artery materials including plaque tissues. The VA model parameter values for layer-specific plaque tissues were then identified through inverse modeling of the tensile experimental data. The VA model was implemented in a general-purpose finite element code [8] via user subroutines, enabling finite element simulations of the uniaxial experiments during the inverse analysis procedure.

2. Material and methods

2.1. Experimental process

In this study, specimens were made of diseased media (DM) and fibrous cap (FC) obtained from human carotid artery after endarterectomies. The experimental setup is similar to the uniaxial tensile tests of porcine abdominal aortas [9, 10]. The diseased media and fibrous cap were isolated, washed in PBS and dissected from the perivascular tissue. One end of the specimen was gripped by a pair of clamps connected to an actuator (Bose ELF 3200, Biodynamic Co, MN), which controlled the sequential loading-unloading cycle. The other end was fixed by a pair of clamps connected to load cell (Bose ELF 3200, Biodynamic Co, MN) for load data recording. The uniaxial tensile loading process was recorded by a microscopic computer vision system which was placed at a fixed distance in the front of the specimen [11], as shown in Figure 1.

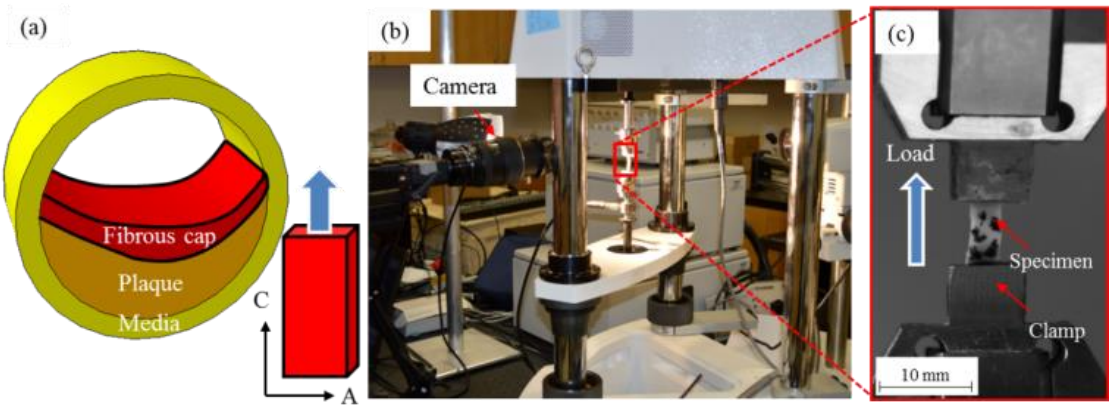

Figure 1. Experimental process: (a) schematic of carotid artery media and fibrous cap specimens obtained from endarterectomies which were cut into strips transversely (A: axial direction; C: circumferential direction); (b) experimental setup of stress relaxation and uniaxial tensile tests; (c) specimen setup (zoomed-in view).

2.2. Theoretical framework

2.2.1. Viscoelastic Anisotropic Model for Soft Material. The constitutive model for describing the arterial tissue is acquired from a decomposition of the stress expressions into three different parts; the viscoelastic stress response (non-equilibrium state) [12], the volumetric part and the isochoric stress response (equilibrium condition).

*2.2.2. Anisotropic Hyperelastic Model: T*he Holzapfel-Gasser-Ogden (HGO) Model. The free energy potential Ψ per unit reference volume of arterial material in a decoupled form is expressed as:

$$\Psi = \frac{1}{D}\left(\frac{J^2-1}{2} - \ln J\right) + \frac{\mu}{2}(\bar{I}_1 - 3) + \frac{k_1}{2k_2}\left[e^{k_2[\kappa\bar{I}_1+(1-3\kappa)\bar{I}_{41}-1]^2} - 1\right] + \frac{k_1}{2k_2}\left[e^{k_2[\kappa\bar{I}_1+(1-3\kappa)\bar{I}_{42}-1]^2} - 1\right] \quad (1)$$

where $\frac{1}{D}$ is analogous to the bulk modulus of the material, $\bar{I}_1 = tr(\bar{\boldsymbol{C}})$ denotes the first invariant of $\bar{\boldsymbol{C}}$, and μ is the neo-Hookean parameter, which characterizes the shear modulus of the material without fibers; $\bar{I}_{41} = \boldsymbol{a}_{01} \cdot \bar{\boldsymbol{C}}\boldsymbol{a}_{01}$ and $\bar{I}_{42} = \boldsymbol{a}_{02} \cdot \bar{\boldsymbol{C}}\boldsymbol{a}_{02}$ are tensor invariants equal to the square of the stretch in the direction of $[\boldsymbol{a}_{01}] = [cos\gamma,\ sin\gamma, 0]$ and $[\boldsymbol{a}_{02}] = [cos\gamma,\ -sin\gamma, 0]$, respectively [13]错误!未定义书签。. The constitutive parameter k_1 is related to the relative stiffness of fibers, which is determined from mechanical tissue experiments; k_2 is a dimensionless stiffness paramter. The parameter κ is the fiber dispersion parameter.

2.2.3. Viscoelastic Anisotropic (VA) Model. A viscoelastic anisotropic (VA) model was developed based on the HGO model [14, 15] by incorporating a viscoelasticity formulation [16]. The second Piola-Kirchhoff stress tensor of VA model $\mathbf{S}_{m+1}$ at time t_{m+1} is given by [17, 18]:

$$S_{m+1} = \left(S_{vol}^{\infty} + S_{g}^{\infty} + + S_{f}^{\infty} + \sum_{\alpha=1}^{n} Q_{\alpha}\right)_{m+1} \tag{2}$$

where "∞" expresses the equilibrium condition when the time approaches infinity.

The non-equilibrium stress tensor $\boldsymbol{Q}_{\alpha\,(m+1)}$ includes mechanical response from matrix material $\boldsymbol{Q}_{g\alpha\,(m+1)}$and fibers $\boldsymbol{Q}_{f\alpha\,(m+1)}$ at time t_{m+1} which are denoted as

$$Q_{g\alpha\,(m+1)} = \exp\left(-\frac{\Delta t}{2T_{g\alpha}}\right)\left[\exp\left(-\frac{\Delta t}{2T_{g\alpha}}\right)Q_{g\alpha\,(m)} - \beta_{g\alpha}\left(S_{g}^{\infty}\right)_{m}\right] + \beta_{g\alpha}\exp\left(-\frac{\Delta t}{2T_{g\alpha}}\right)\left(S_{g}^{\infty}\right)_{m+1} \tag{3}$$

$$Q_{f\alpha\,(m+1)} = \exp\left(-\frac{\Delta t}{2T_{f\alpha}}\right)\left[\exp\left(-\frac{\Delta t}{2T_{f\alpha}}\right)Q_{f\alpha\,(m)} - \beta_{g\alpha}\left(S_{f}^{\infty}\right)_{m}\right] + \beta_{f\alpha}\exp\left(-\frac{\Delta t}{2T_{f\alpha}}\right)\left(S_{f}^{\infty}\right)_{m+1} \tag{4}$$

The Cauchy stress tensor σ_{m+1} at time t_{m+1}

$$\sigma_{m+1} = \left(J^{-1}FSF^{T}\right)_{m+1} \tag{5}$$

In the above equations, Δt is the time increment from time t_m to t_{m+1}; $T_{g\alpha}$ $(\alpha = 1\sim n)$ and $T_{f\alpha}$ represent the relaxation time for ground matrix material and collagen fibers, respectively. In addition, $\beta_{g\alpha}$ and $\beta_{f\alpha}$ denote the non-dimensional parameter for ground matrix material and fibers, respectively. For the finite element analyses, a single set of viscoelastic parameters such as T_{g1}, β_{g1}, T_{f1} and β_{f1} $(\alpha = 1)$ was used.

3. Inverse analysis method

Inverse analysis utilizes the history of variables (e.g., force, displacement and stress) measured in an experiment (e.g., uniaxial tensile loading) to identify a set of model parameter values for the test. This set of parameter values can be used in a model of the experiment to predict the history of the variables that provide a best fit to the measured history according to an error minimization criterion [19, 20]. In the current study, the objective function in the error minimization criterion describes the difference between the predicted and measured force history and is given by

$$f(\mu, k_1, k_2, \gamma, \kappa, T_{g1}, \beta_{g1}, T_{f1}, \beta_{f1}) = \sum_{i=1}^{n}[F_{p_i}(\mu, k_1, k_2, \gamma, \kappa, T_{g1}, \beta_{g1}, T_{f1}, \beta_{f1}) - F_{e_i}]^2 \tag{6}$$

where $F_{p_i}(\mu, k_1, k_2, \gamma, \kappa, T_{g1}, \beta_{g1}, T_{f1}, \beta_{f1})$ and F_{e_i} are predicted and measured force data, respectively, at the *i*th increment. A reasonable set of parameters values was obtained when the objective function is minimized to an acceptable value.

4. Numerical implementation

In order to identify the VA model material parameters for the human carotid plaque tissue, inverse modeling of the uniaxial experiment was used to automatically predict and compare the load-displacement data with the experimental measurements. A set of converged parameter values were acquired when the objective function diminished to a small value and the convergence criteria was met (Figure 2).

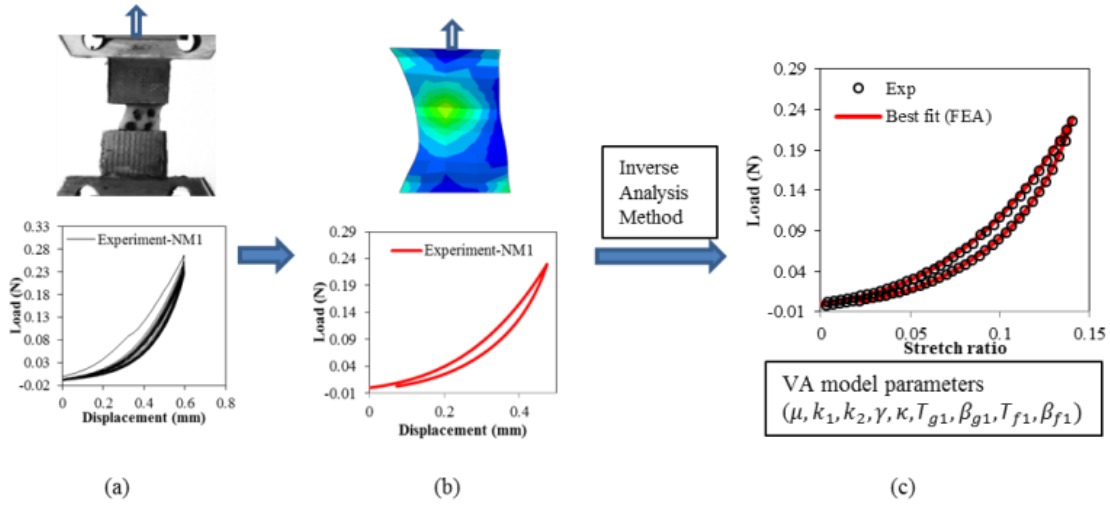

Figure 2. Schematic procedure of the inverse modeling of arterial tissue: (a) uniaxial tensile test and the load-displacement curves from the test; (b) FE model of the test and the predicted load-displacement curves with certain model parameter values; (c) best fit between predicted and measured load-displacement curves, resulting in the identified model parameter values.

5. Results

The data of load vs. stretch ratio from uniaxial tensile tests were used for identification of material parameters of VA model. The material parameter values of VA model, Eq. (5), were obtained from the best fit between experimental and simulation results through inverse analysis method, which is shown in Figure 3. The parameter values for samples of diseased media and fibrous cap are shown in Table 1 and Table 2, respectively.

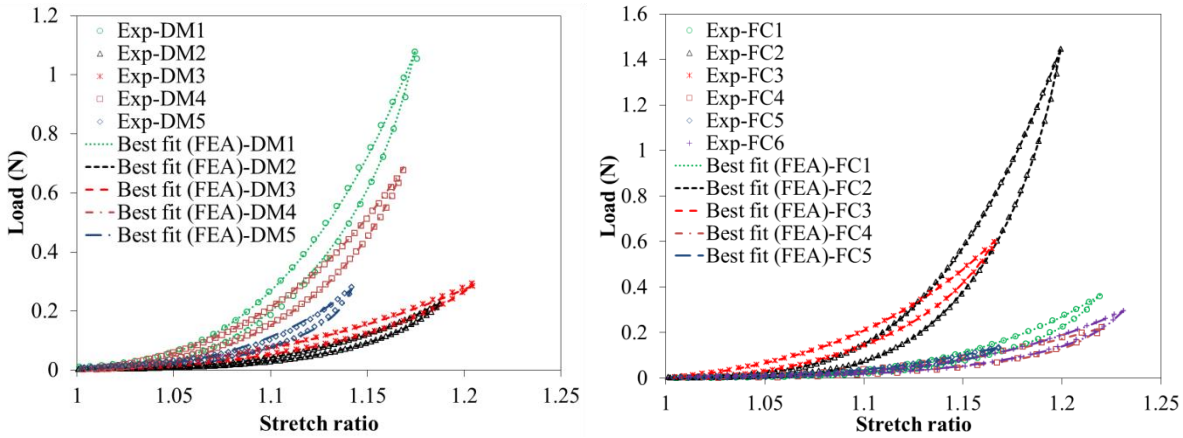

Figure 3. Comparisons between experimental and best fit (inverse analysis method) results of uniaxial tensile tests for five human diseased media (DM) and six human fibrous cap (FC) samples.

In our study, the viscoelastic response is well captured through a matrix-fibers linear viscoelastic anisotropic model, in which the parameters (μ, k_1, k_2, γ and κ) represent the anisotropic hyperelastic behavior of the arterial tissue, and the remaining parameters (T_{g1}, β_{g1}, T_{f1} and β_{f1}) characterize the viscoelastic response from the matrix material and the collagen fibers. The material parameters obtained from the loading-unloading cycle of uniaxial experiments are diversely distributed which may be attributed to sample variability among individual patients.

Table 1. Best-fit parameter values for the viscoelastic anisotropic (VA) model of human diseased media samples under uniaxial tensile tests.

Sample	μ (kPa)	k_1 (kPa)	k_2	γ (angle)	κ	T_{g1}	β_{g1}	T_{f1}	β_{f1}	Residual
DM1	0.04	3010.00	36.80	50.08	0.31	0.18	0.02	1.07	0.43	0.00057
DM2	0.12	3610.00	81.11	48.75	0.31	0.18	0.02	1.36	0.53	0.00011
DM3	1.17	650.00	0.02	41.85	0.21	0.18	0.02	1.97	0.41	0.00001
DM4	0.03	2470.00	33.69	61.22	0.30	0.18	0.02	1.97	0.41	0.00009
DM5	0.01	6230.00	100.00	57.03	0.32	0.18	0.02	0.75	1.11	0.00065
Average	0.27	3194.00	50.32	51.79	0.29	0.18	0.02	1.42	0.58	0.00029
SD	0.45	1812.20	35.79	6.74	0.04	0.00	0.00	0.49	0.27	0.00027

Table 2. Best-fit parameter values for the viscoelastic anisotropic (VA) model of human fibrous cap samples under uniaxial tensile tests.

Sample	μ (kPa)	k_1 (kPa)	k_2	γ (angle)	κ	T_{g1}	β_{g1}	T_{f1}	β_{f1}	Residual
FC1	0.30	2333.00	72.43	30.89	0.33	0.18	0.02	1.08	0.54	0.000569
FC2	1.04	5570.00	13.02	30.84	0.27	0.01	2.92	1.84	0.61	0.000114
FC3	1.05	1370.70	21.37	43.57	0.21	5.17	1.39	1.50	0.45	0.000032
FC4	1.15	479.00	13.96	36.33	0.25	0.34	1.20	0.69	1.09	0.000003
FC5	0.60	512.00	17.39	41.17	0.20	1.57	2.73	0.54	1.23	0.000009
FC6	0.80	1451.00	2.81	24.55	0.26	0.12	7.08	0.77	0.84	0.000138
Average	0.82	1952.62	23.50	34.56	0.25	1.23	2.56	1.07	0.79	0.000144
SD	0.30	1735.29	22.60	6.53	0.04	1.84	2.25	0.46	0.29	0.000197

6. Conclusion

The aim of this study was to characterize the viscoelastic properties of human carotid artery atherosclerotic plaque tissues. The passive viscoelastic responses were manifested in terms of the load-stretch curves for loading-unloading cycles in uniaxial tensile tests. The VA model parameter values were identified through an automated inverse analysis procedure by matching finite element simulation predictions with experimental measurements of the observed viscoelastic responses from the uniaxial tensile tests. The proposed VA model, along with the identified model parameter values, will enable solutions of boundary-value problems in terms of predicting arterial mechanical responses and arterial wall stress distributions under various loading scenarios.

Several sources of approximations were involved in the current study. The test sample geometry models were reconstructed from images of front and side views of the samples, assuming the sample thicknesses is constant along the sample width direction. Secondly, the samples under uniaxial tensile test did not undergo pure tensile deformation because shearing forces may occur inside the samples with large width-length ratio. Thirdly, the material parameter values identified from this study were identified from a single stretch ratio which may not fully characterize the mechanical behavior of the arterial tissue.

7. Acknowledgments

The authors gratefully acknowledge the sponsorship of NSF (award # CMMI-1200358) and this work was partially supported by a SPARC Graduate Research Grant from the Office of the Vice President for Research at the University of South Carolina.

8. References

[1] Badimon L, Vilahur G. Thrombosis formation on atherosclerotic lesions and plaque rupture. Journal of Internal Medicine 2014; 276: 618- 32.

[2] Prim DA, Zhou B, Hartstone-Rose A, Uline MJ, Shazly T, Eberth JF. A mechanical argument for the differential performance of coronary artery grafts. Journal of the mechanical behavior of biomedical materials 2016; 54: 93-105.
[3] Zareh M, Fradet G, Naser G, Mohammadi H. Are two-dimensional images sufficient to assess the atherosclerotic plaque vulnerability: a viscoelastic and anisotropic finite element model 2015.
[4] Antonova ML, Antonov PS, Marinov GR, Vlaskovska MV, Kasakov LN. Viscoelastic characteristics of in vitro vital and devitalized rat aorta and human arterial prostheses. Annals of biomedical engineering 2008; 36: 947-57.
[5] Hemmasizadeh A, Autieri M, Darvish K. Multilayer material properties of aorta determined from nanoindentation tests. Journal of the Mechanical Behavior of Biomedical Materials 2012; 15:199- 207.
[6] Holzapfel GA, Gasser TC, Ogden RW. A New Constitutive Framework for Arterial Wall Mechanics and a Comparative Study of Material Models. Journal of elasticity and the physical science of solids 2000; 61: 1-48.
[7] Gasser T, W Ogden R, Holzapfel G. Hyperelastic modeling of arterial layers with distributed collagen fibre orientations2006.
[8] ABAQUS. Analysis user's manual version 6.12, Dassault Systemes Corp. 2013.
[9] Leng X, Zhou B, Deng X, Davis L, Lessner SM, Sutton MA, et al. Experimental and numerical studies of two arterial wall delamination modes. Journal of the Mechanical Behavior of Biomedical Materials 2018; 77: 321-30.
[10] Shazly T, Rachev A, Lessner S, Argraves WS, Ferdous J, Zhou B, et al. On the uniaxial ring test of tissue engineered constructs. Experimental Mechanics 2015; 55: 41-51.
[11] Zhou B, Ravindran S, Ferdous J, Kidane A, Sutton MA, Shazly T. Using digital image correlation to characterize local strains on vascular tissue specimens. JoVE (Journal of Visualized Experiments) 2016: e53625- e.
[12] Holzapfel GA, Gasser TC, Stadler M. A structural model for the viscoelastic behavior of arterial walls: Continuum formulation and finite element analysis. European Journal of Mechanics - A/Solids 2002; 21: 441-63.
[13] Zhou B, Rachev A, Shazly T. The biaxial active mechanical properties of the porcine primary renal artery. Journal of the mechanical behavior of biomedical materials 2015; 48: 28-37.
[14] Gasser TC, Ogden RW, Holzapfel GA. Hyperelastic modelling of arterial layers with distributed collagen fibre orientations. Journal of the Royal Society, Interface / the Royal Society 2006; 3:15-35.
[15] Zhou B, Alshareef M, Prim D, Collins M, Kempner M, Hartstone-Rose A, et al. The perivascular environment along the vertebral artery governs segment-specific structural and mechanical properties. Acta biomaterialia 2016; 45: 286- 95.
[16] Holzapfel GA, Gasser TC. A viscoelastic model for fiber-reinforced composites at finite strains: Continuum basis, computational aspects and applications. Computer Methods in Applied Mechanics and Engineering 2001; 190: 4379- 403.
[17] Holzapfel GA. Nonlinear Solid Mechanics. A Continuum Approach for Engineering. John Wiley & Sons, Chichester 2000.
[18] Unterberger MJ, Schmoller KM, Wurm C, Bausch AR, Holzapfel GA. Viscoelasticity of cross-linked actin networks: experimental tests, mechanical modeling and finite-element analysis. Acta biomaterialia 2013; 9: 7343-53.
[19] Lei F, Szeri AZ. Inverse analysis of constitutive models: Biological soft tissues. Journal of biomechanics 2007; 40: 936-40.
[20] Zhou B, Wolf L, Rachev A, Shazly T. A structure-motivated model of the passive mechanical response of the primary porcine renal artery. Journal of Mechanics in Medicine and Biology 2014; 14: 1450033.